Appl. Numer. Math. 207 (2025) 323–338

Contents lists available at ScienceDirect

Applied Numerical Mathematics

journal homepage: www.elsevier.com/locate/apnum

Research Paper

A comparative study on numerical methods for Fredholm integro-differential equations of convection-diffusion problem with integral boundary conditions

Sekar Elango [a], L. Govindarao [a,*], R. Vadivel [b]

[a] Department of Mathematics, Amrita School of Physical Science, Coimbatore, Amrita Vishwa Vidyapeetham, India
[b] Department of Mathematics, Faculty of Science and Technology, Phuket Rajabhat University, Phuket, 83000, Thailand

A R T I C L E I N F O

Keywords:
Singular perturbation
Convection-diffusion
Integral boundary conditions
Boundary layer
Hybrid scheme
Error estimation

A B S T R A C T

This paper numerically solves Fredholm integro-differential equations with small parameters and integral boundary conditions. The solution of these equations has a boundary layer at the right boundary. A central difference scheme approximates the second-order derivative, a backward difference (upwind scheme) approximates the first-order derivative, and the trapezoidal rule is used for the integral term with a Shishkin mesh. It is shown that theoretically, the proposed scheme is uniformly convergent with almost first-order convergence. Further to improve the order of convergence from first order to second order, we use the post-processing and the hybrid scheme. Two numerical examples are computed to support the theoretical results.

1. Introduction

Fredholm integro-differential equations (FIDEs) are fundamental in many scientific domains, including engineering, biology, physics, chemistry, potential theory, electrostatics, finance, theory of elasticity, fluid dynamics, astronomy, economics, and heat-mass transfer (e.g., [4,37,48]). However, finding the solutions to such types of equations is extremely difficult. Numerical approaches are crucial in tackling these difficulties, as seen in [4,7,8,14,37,48,18,56,59]. As an example, we illustrate the convection-diffusion parabolic partial integro-differential equation [31,55] provided as

$$u_t(s,t) + cu_s(s,t) - du_{ss}(s,t) = \int_0^t K(q-t)u(s,q)dq + f(s,t),$$

with $u(s,0) = g(s),\ \ s \in (a,b)$ and $y(a,t) = g_1(t),\ y(b,t) = g_2(t),\ t > 0$, where the integral term is known as the memory term and $g(s)$, $g_1(t)$, and $g_2(t)$ are known functions.

Suppose that the highest derivative term in differential equations (DEs) is multiplied by a small parameter $0 < \varepsilon << 1$ then the parameter is called a singularly perturbation parameter and the DEs are known as singularly perturbed differential equations (SPDEs).

* Corresponding author.
E-mail address: l_govindarao@cb.amrita.edu (L. Govindarao).

https://doi.org/10.1016/j.apnum.2024.09.001
Received 6 March 2024; Received in revised form 29 July 2024; Accepted 1 September 2024

Available online 13 September 2024
0168-9274/

Solutions to these problems possess boundary layers which are thin regions in the neighborhood of the boundary of the domain due to the perturbation parameter's existence.

These SPDEs have several applications in biology, ecology, physical sciences, and other fields. For example, the following equation governs the one-dimensional groundwater flow and solute transport problem,

$$y_t(s,t) = \varepsilon z_{ss}(s,t) - \upsilon y_x(s,t) - \lambda y(s,t),\ s > 0,\ t > 0.$$

It illustrates how water and solutes travel across the unsaturated zone [24], where the duration is t and the horizontal distance is s, both positive and measurable.

Furthermore, polymer rheology, population dynamics, and mathematical models of glucose tolerance all employ singularly perturbed integro-differential equations (SPIDEs) [3,15,16,23,38,42,60]. Authors in [47] discussed optimal control problems mostly utilizing singularly perturbed Fredholm integro-differential equations (SPFIDEs). Some asymptotic solutions to this problem were described in [41] and [46,47]. For example, authors in [35] describe a class of singularly perturbed partial integro-differential equations in viscoelasticity as

$$\rho u^{\rho}_{tt}(t,x) = \varepsilon u^{\rho}_{xx}(t,x) + \int_{-\infty}^{t} a(t-s) u^{\rho}_{ss}(s,x)ds + \rho g(t,x) + f(x).$$

However, the theory and approximate numerical solutions for SPIDEs are still in their early stages. In recent years, many numerical approaches have been presented for first-order SPIDEs without integral boundary conditions on uniform and non-uniform meshes, as shown in [1,2,5,13,21,22,29,39,43]. The article [6,19,25–28,61] discusses second-order SPIDEs on Shishkin meshes without non-local boundary conditions. Higher-order numerical methods for SPDEs are considered in [9,11,12,17,20,57]. One can refer [19] for the layer is varying in the interior part of the domain. Several problems on singularly perturbed delay differential equations with integral boundary conditions are discussed in [10,49–52]. Numerical approaches for first-order SPFIDEs with beginning and integral boundary conditions (IBCs) on Shishkin meshes are in [29]. In [30,33] discussed SPIDEs with reaction-diffusion problem and they proved second order rate of convergence. Motivated by the preceding work, we analyze an efficient numerical method for second-order SPIDEs convection-diffusion problems with IBCs on Shishkin mesh. This article aims to solve numerically a class of singularly perturbed convection-diffusion Fredholm integro-differential equation with integral boundary conditions provided as

$$\begin{aligned} &Lu := L_1 u + L_2 u = f(x),\ x \in \Omega = (0,1), \\ &\mathcal{K}u(0) := u(0) - \varepsilon \int_0^1 g_1(x)u(x)dx = l, \\ &\mathcal{K}u(1) := u(1) - \varepsilon \int_0^1 g_2(x)u(x)dx = r, \end{aligned} \tag{1.1}$$

where $L_1 u = -\varepsilon u'' + a(x)u' + b(x)u$, $L_2 u = -\lambda \displaystyle\int_0^1 K(x,s)u(s)ds$ and $\gamma > K(x,s) \in L^2[0,1]$. It is assumed that $a(x) \geq \alpha_1 > \alpha > 0$, $b(x) \geq \beta > \lambda\gamma > 0$, where λ and γ are positive constants and $\int_0^1 g_i(x)dx < 1, i = 1,2$, $g_i(x)$ are non-negative sufficiently smooth functions satisfying appropriate regularity conditions.

In this article, the problem (1.1) is solved using a central difference scheme for approximating the second-order derivative and the composite trapezoidal rule for approximating an integral part of the Shishkin mesh. The proposed method provides an optimal at most first-order rate of convergence $\left(CN^{-1}\ln^2 N\right)$, then using the extrapolation technique and hybrid difference method, a second-order rate of convergence $\left(CN^{-2}\ln^2 N\right)$ is obtained.

The article is organized as follows: In Section 2, we present an analysis of the analytical solution, maximum principle and stability results. Section 3 constructs the Shishkin mesh and the computational analysis for the finite difference scheme. Section 4 introduces the Richardson extrapolation and the corresponding convergence analysis. Section 5 is discussed in convergence analysis for the hybrid difference scheme. Section 6 presents some numerical examples with graphs and tables to show the performance of the proposed methods. Finally, Section 7 summarizes the article's conclusions. Throughout our analysis, we consider C and C_1 to be any positive constant independent of ε. The standard supremum norm, $||\mathfrak{f}||_{\mathfrak{D}} = \sup_{y\in\mathfrak{D}} |\mathfrak{f}(y)|$, on a given domain $\mathfrak{D}$.

2. Analysis on continuous solution

Theorem 2.1. *Let $\psi(x)$ be any function such that $\mathcal{K}\psi(0) \geq 0$, $\mathcal{K}\psi(1) \geq 0$ and $L\psi(x) \geq 0$, $\forall x \in \Omega$, where $\mathcal{K}$ and the differential operator L are defined in (1.1). Then $\psi(x) \geq 0$, $\forall x \in \overline{\Omega} = [0,1]$.*

Proof. Consider the function $s(x) = 1 + x$, which is non negative for $x \in \overline{\Omega}$. Let us consider

$$\mu = \max\left\{ \frac{-\psi(x)}{s(x)} : x \in \overline{\Omega} \right\}.$$

If $x_0 \in \overline{\Omega}$, $\psi(x_0) + \mu s(x_0) = 0$ exists, and thus, for any $x \in \overline{\Omega}$, $\psi(x) + \mu s(x) \geq 0$. Consequently, $x = x_0$ is where the function $(\psi + \mu s)$ reaches its minimum. Suppose the theorem does not hold true, then it is $\mu > 0$. Now, consider two cases:

Case (i): $x_0 = 0$ or $x_0 = 1$;

Note that $\mathcal{K}(\psi + \mu s)(x_0) = \mathcal{K}\psi(x_0) + \mu\mathcal{K}s(x_0) > 0$. On the other hand, it is

$$\mathcal{K}(\psi + \mu s)(x_0) = (\psi + \mu s)(x_0) - \varepsilon \int_0^1 g_1(x)(\psi + \mu s)(x)dx,$$

$$= -\varepsilon \int_0^1 g_1(x)(\psi + \mu s)(x)dx \leq 0.$$

Case (ii): $x_0 \in \Omega$;

Clearly $L\psi(x_0) \geq 0$, then

$$L_1(\psi + \mu s)(x_0) = -\varepsilon(\psi + \mu s)''(x_0) + a(x_0)(\psi + \mu s)'(x_0) + b(x_0)(\psi + \mu s)(x_0),$$

$$= -\varepsilon(\psi + \mu s)''(x_0) + b(x_0)(\psi + \mu s)(x_0) \leq 0,$$

$$L_2(\psi + \mu s)(x_0) = -\lambda \int_0^1 K(x, s)(\psi + \mu s)(s)ds \leq 0.$$

Then,

$$0 < L(\psi + \mu s)(x_0) = L_1(\psi + \mu s)(x_0) + L_2(\psi + \mu s)(x_0) \leq 0,$$

and thus, we arrive at a contradiction. □

Theorem 2.2. *Let $u(x)$ be the solution of problem (1.1). Then, the following bounds of the solution and its derivatives hold:*

(i) $||u|| \leq C \max_{x\in\Omega} \left\{ |\mathcal{K}u(0)|, |\mathcal{K}u(1)|, |Lu(x)| \right\}$. *(***Stability Result***).*
(ii) $||u^{(k)}|| \leq C\varepsilon^{-k}$, *for* $k = 1, 2, 3, 4$.

Proof. Proof is available in [50]. □

Lemma 2.3. *Let us consider the decomposition of the solution $u(x)$ of the problem (1.1) in the form $u = v + w$, where v is smooth and w is singular components. Then, it holds for $k = 0, 1, 2, 3, 4$ that*

(i) $|v^{(k)}(x)| \leq C(1 + \varepsilon^{-(2-k)})$.
(ii) $|w^{(k)}(x)| \leq C\varepsilon^{-k}e^{-\alpha(1-x)/\varepsilon}$.

Proof. (i) The proof is available in [50].

(ii) Consider $\psi^{\pm}(x) = Ce^{-\alpha(1-x)/\varepsilon} \pm w(x)$, then

$$\mathcal{K}\psi^{\pm}(0) = C \pm w(0) - \varepsilon \int_0^1 g_1(x)(Ce^{-\alpha(1-x)/\varepsilon} \pm w(x))dx,$$

$$= C(1 - \varepsilon \int_0^1 g_1(x)e^{-\alpha(1-x)/\varepsilon}dx) \pm \mathcal{K}w(0) \geq 0.$$

$$\mathcal{K}\psi^{\pm}(1) = C \pm w(1) - \varepsilon \int_0^1 g_2(x)(Ce^{-\alpha(1-x)/\varepsilon} \pm w(x))dx,$$

$$= C(1 - \varepsilon \int_0^1 g_2(x)e^{-\alpha(1-x)/\varepsilon}dx) \pm \mathcal{K}w(1) \geq 0.$$

$$L\psi^{\pm}(x) = Ce^{-\alpha(1-x)/\varepsilon}\Big[(\alpha/\varepsilon)(a(x) - \alpha) + b(x)\Big] - \lambda \int_0^1 CK(x, s)e^{-\alpha(1-x)/\varepsilon}ds \pm Lw(x),$$

$$\geq Ce^{-\alpha(1-x)/\varepsilon}\Big[(\alpha/\varepsilon)(\alpha_1-\alpha)+\beta-\lambda\gamma\Big]\geq 0.$$

Using Theorem 2.1, then $\psi^{\pm}(x)\geq 0$ and thus

$$|w(x)|\leq Ce^{-\alpha(1-x)/\varepsilon}.$$

For the derivative bounds of regular component, the proof is the same as in [44], resulting in

$$|w^{(k)}(x)|\leq C\varepsilon^{-k}e^{-\alpha(1-x)/\varepsilon}. \quad \square$$

3. Numerical scheme and analysis

Shishkin mesh (S-mesh):

The transition parameter σ is defined as $\sigma=\min\left\{\frac{1}{2},\frac{\varepsilon}{\alpha}\ln(N)\right\}$. More details about the S-mesh can be found in [44,53]. The mesh points are defined as $\bar{\Omega}^N=\{x_0,x_1,x_2,\dots,x_N\}\in[0,1]$, where

$$x_i=\begin{cases} iH_1, & \text{for} \quad i=0,\dots,\frac{N}{2},\\ x_{\frac{N}{2}}+iH_2, & \text{for} \quad i=\frac{N}{2}+1,\dots,N,\end{cases}$$

with $H_1=\frac{2\sigma}{N}$, $H_2=\frac{2(1-\sigma)}{N}$. The step sizes in the space variable are given as $h_i=x_i-x_{i-1}$, for $i=0,1,\dots,N$.

3.1. Upwind scheme (M1)

Given a mesh function ϕ_i, the backward, forward, and center difference operators are defined as follows:

$$D_x^+\phi_i=\frac{\phi_{i+1}-\phi_i}{h_{i+1}},\quad D_x^-\phi_i=\frac{\phi_i-\phi_{i-1}}{h_i},\quad D_x^0\phi_i=\frac{\phi_{i+1}-\phi_{i-1}}{h_{i+1}+h_i},$$

respectively and the approximate second-order operator is given as

$$D_x^+D_x^-\phi_i=\frac{2}{h_i+h_{i+1}}\left(\frac{\phi_{i+1}-\phi_i}{h_{i+1}}-\frac{\phi_i-\phi_{i-1}}{h_i}\right),$$

where $\phi_i=\phi(x_i)$.

We discretize the problem (1.1) using the upwind method (the central difference scheme for the second-order derivative and backward difference approximation for the first derivative) and the trapezoidal method for the integral part as similar to [30,33]. The proposed numerical scheme is given as follows:

$$\begin{cases}\left(L_1^N+L_2^N\right)U_i=f_i, \ \text{for} \quad i=1,\dots,N-1,\\ \mathcal{K}^NU_0=U_0-\varepsilon\sum\limits_{i=1}^{N}\frac{g_{i-1}Ui-1+g_iU_i}{2}h_i,\\ \mathcal{K}^NU_N=U_N-\varepsilon\sum\limits_{i=1}^{N}\frac{g_{i-1}Ui-1+g_iU_i}{2}h_i,\end{cases} \tag{3.1}$$

where,

$$L_1^NU_i=-\varepsilon D_x^+D_x^-U_i+a_iD_x^-U_i+b_iU_i,\quad L_2^NU_i=-\lambda\sum_{j=0}^{N}\tau_jK_{i,j}U_i,$$

$$\tau_0=\frac{h_0}{2},\ \tau_j=\frac{h_j+h_{j+1}}{2},\ \ j=1,2,\dots,N-1,\ \tau_N=\frac{h_N}{2},$$

$U_i=U(x_i)$ is the approximate solution to the exact solution of the problem (1.1), $a_i=a(x_i)$, $f_i=f(x_i)$, $K_{i,j}=K(x_i,s_j)$ and $\left\{x_i\right\}$ are the grid points considered.

The following result is a discrete version of Theorem 2.1 and the proof can be obtained similarly.

Theorem 3.1. *Given any discrete function $\psi(x_i)$ on a mesh $\left\{x_i\right\}_{i=1}^{N}$ such that $\mathcal{K}^N\psi(x_0)\geq 0$, $\mathcal{K}^N\psi(x_N)\geq 0$ and $L^N\psi(x_i)\geq 0$ then $\psi(x_i)\geq 0$, $\forall x_i\in\overline{\Omega}^N$.*

Proof. Consider $s(x_i) = 1 + x_i$. Note that the function is non-negative on $x_i \in \overline{\Omega}^N$. Let

$$\mu = \max\left\{ \frac{-\psi(x_i)}{s(x_i)} : x_i \in \overline{\Omega}^N \right\}.$$

Furthermore, $\exists\, x_k \in \overline{\Omega}^N$ such that $\psi(x_k) + \mu s(x_k) = 0$ and $\psi(x_i) + \mu s(x_i) \geq 0, \forall x_i \in \overline{\Omega}^N$. As a result, at $x = x_k$, the function $(\psi + \mu s)$ attains its minimum. If the theorem is false, then it is $\mu > 0$.
Case (i): $x_k = x_0$ or $x_k = x_N$. Then

$$0 < \mathcal{K}^N(\psi + \mu s)(x_k) = (\psi + \mu s)(x_k) - \varepsilon \sum_{i=1}^{N} \frac{g_{i-1}(\psi + \mu s)x_{i-1} + g_i(\psi + \mu s)x_i}{2} h_i \leq 0.$$

Case (ii): If $x_k \in \Omega^N$, then

$$0 < L_1(\psi + \mu s)(x_k) = -\varepsilon D_x^+ D_x^-(\psi + \mu s)(x_k) + a(x_k) D_x^-(\psi + \mu s)(x_k) + b(x_k)(\psi + \mu s)(x_k) \leq 0.$$

$$\begin{aligned} 0 < L_2(\psi + \mu s)(x_k) &= -\lambda \Big[h_1 k_{i,1}(\psi + \mu s)_1 + \cdots + h_N k_{i,N}(\psi + \mu s)_N \Big], \\ &\leq -\lambda(\psi + \mu s)_k \Big[h_1 k_{i,1} + \cdots + h_N k_{i,N} \Big] \leq 0. \end{aligned}$$

The contradiction arrived in the above cases. □

Theorem 3.2. *If ϕ_i is any mesh function, then*

$$\left|\phi_i\right| \leq \max_{1\leq j\leq N-1} \left\{ |L^N \phi_j|, |\mathcal{K}^N \phi_0|, |\mathcal{K}^N \phi_N| \right\}, \text{ for } 0 \leq i \leq N.$$

Proof. One can prove this easily as using Theorem 3.1. □

Theorem 3.3. *Let $U(x_i)$ be a numerical solution of (3.1) defined as (1.1) and $V(x_i)$ is a numerical solution of the regular problem. Then*

$$|U(x_i) - V(x_i)| \leq C \begin{cases} N^{-1}, & i = 0, 1, ..., \frac{3N}{4} \\ N^{-1} + |r - V(x_N)|, & i = \frac{3N}{4} + 1, ..., N. \end{cases}$$

Proof. Consider the barrier functions

$$\theta^{\pm}(x_i) = C_1 N^{-1} s(x_i) + C_1 x_i \Psi(x_i) \pm (U(x_i) - V(x_i)), \forall x_i \in \overline{\Omega}^N,$$

$$\text{where } \Psi(x_i) = \begin{cases} 0, & i = 0, 1, ..., \frac{3N}{4}, \\ |r - V(x_N)|, & i = \frac{3N}{4} + 1, ..., N. \end{cases}$$

It is clear that $\theta^{\pm}(x_0) \geq 0$ and $\theta^{\pm}(x_N) \geq 0$.

$$\mathcal{L}^N \theta^{\pm}(x_i) \geq 0, \text{ for all } i \in \{1, 2, ..., N-1\}.$$

Using Theorem 3.1, this theorem gets proved. □

3.2. Error estimate for the difference schemes

Error estimates are bound by the error of the numerical solution. The discrete maximum norm is a measure of the error that takes the maximum absolute value of the errors at the mesh points. Formally, if u is the exact solution and U^N is the numerical solution on a mesh with parameter N, then the discrete maximum norm of the error is $\|(u - U^N)(x_i)\|_\infty = \max |u(x) - U^N(x_i)|$ for all mesh points x_i.

Theorem 3.4. *Given u and U^N, which are respectively the solutions to (1.1) and (3.1), we get the following estimate of the numerical errors (3.1)*

$$\max_{1\leq i\leq N-1} \left|(u - U^N)(x_i)\right| \leq C N^{-1} (\ln N)^2.$$

Proof. It is possible to separate the discrete solution U into singular (W) and smooth (V) components. The error can be written in the form

$$L^N(U - u) = L_1^N(U - u) + L_2^N(U - u).$$

From [50], we have

$$L_1^N(U-u) \le CN^{-1}(\ln N)^2.$$

Next, for the L_2 operator the bound is

$$L_2^N(U-u) = L_2^N(V-v) + L_2^N(W-w) \le CN^{-1}(\ln N)^2.$$

Now, we examine the smooth and singular component bounds as follows.

Smooth components:

$$\begin{aligned}
L_2^N(V_i - v_i) &= L_2^N(V(x_i)) - L_2^N(v(x_i)),\\
&= \lambda \sum_{j=0}^{N} K_{ij}V_j - \lambda \int_0^1 K(x,s)v(s)ds,\\
&= \lambda \sum_{j=0}^{N} K_{ij}V_j - \lambda \int_0^1 K(x_i,s_i)v(s_i)ds,\\
&\le C\sum_{j=1}^{N} \int_{x_{j-1}}^{x_j} (x_j-\xi)(\xi - x_{j-1})(1+|v'(\xi)|+|v''(\xi)|)d\xi,\\
&\le C\sqrt{\varepsilon}(h),\\
&\le CN^{-1}.
\end{aligned}$$

At the points $x_k = x_0$ and $x_k = x_N$, then

$$\begin{aligned}
\mathcal{K}^N(V-v)(x_k) &= \mathcal{K}^N V(x_k) - \mathcal{K}^N v(x_k),\\
&= l - \mathcal{K}^N v(x_k),\\
&= \mathcal{K}v(x_k) - \mathcal{K}^N v(x_k),\\
&= v(x_k) + \varepsilon \int_{x_0}^{x_k} g(x)v(x)dx - v(x_N) - \varepsilon \sum_{i=1}^{N} \frac{g_{i-1}v_{i-1} + g_i v_i}{2} h_i,\\
|\mathcal{K}^N(V-v)(x_N)| &\le C\varepsilon((h_1^3 v''(\chi_1) + \cdots + h_N^3 v''(\chi_N)),\\
&\le C\varepsilon(h_1^3 + \cdots + h_N^3),\\
&\le CN^{-1}, \quad \text{where } \ x_{i-1} \le \chi_i \le x_i, 1 \le i \le N.
\end{aligned}$$

Using Theorem 2.2 gives

$$|V(x_i) - v(x_i)| \le CN^{-1}.$$

Singular components:
Take note of this

$$|w(x_i) - W(x_i)| \le |u(x_i) - U(x_i)| + |v(x_i) - V(x_i)|.$$

Next, using Theorem 3.3 and Lemma 2.3, we obtain

$$|u(x_i) - U(x_i)| \le |U(x_i) - V(x_i)| + |v(x_i) - V(x_i)| + |u(x_i) - v(x_i)|.$$

Now,

$$\begin{aligned}
|w(x_i) - W(x_i)| &\le |U(x_i) - V(x_i)| + 2|v(x_i) - V(x_i)| + |u(x_i) - v(x_i)|,\\
&\le C_1 N^{-1} + C_1 \exp(\frac{-\alpha(1-x)}{\varepsilon}) + \varepsilon,\\
&\le C_1 \exp(\frac{-\alpha\sigma}{\varepsilon}) + C_1 N^{-1} \le CN^{-1}, i = 0 \text{ to } \frac{3N}{4}.
\end{aligned} \tag{3.2}$$

Let

$$\phi^{\pm}(x_i) = C_1 N^{-1} s(x_i) + C_1 N^{-1}\frac{\sigma}{\varepsilon^2}(x_i - (1-\sigma)) \pm (w(x_i) - W(x_i)) \quad x_i \in [1-\sigma, 1] \cap \overline{\Omega}^N.$$

Where $s(x_i) = x_i + 1$, note that $\mathcal{K}\phi^{\pm}(x_{\frac{3N}{4}}) \ge 0$ and $\mathcal{K}\phi^{\pm}(x_N) \ge 0$.

$$L^N\phi^{\pm}(x_i) = C_1N^{-1}[a(x_i)+b(x_i)] + C_1N^{-1}\frac{\sigma}{\varepsilon^2}[a(x_i)+b(x_i)(x_i+\sigma-1) - \lambda\sum_{j=0}^{N}\tau_j K_{i,j}\phi^{\pm}(x_i)]$$
$$\pm(\mathcal{L}^N-\mathcal{L})w(x_i),$$
$$\geq C_1N^{-1}[\alpha+\beta-\lambda\gamma_1] + C_1N^{-1}\frac{\sigma}{\varepsilon^2}[\alpha+(\beta-\lambda\gamma_1)(x_i+\sigma-1)] \pm 0,$$
$$\geq 0.$$

Then, $\phi^{\pm}(x_i)\geq 0,\ \forall x_i\in\overline{\Omega}^N$, according to Theorem 3.2. Consequently

$$|w(x_i)-W(x_i)| \leq CN^{-1}ln^2N, \quad x_i\in\overline{\Omega}^N.$$

Therefore,

$$|U(x_i)-u(x_i)| = |V(x_i)-v(x_i)| + |W(x_i)-w(x_i)| \leq CN^{-1}\ln^2 N. \quad \square$$

4. Post-process technique (M2)

We use the Richardson extrapolation approach to improve the accuracy of the proposed scheme. The discrete problem (3.1) is first solved on the S-mesh $\mathbb{G}^{2N}$, which is obtained by bisecting each mesh interval of $\mathbb{G}^N$ and having the same transition point as $\mathbb{G}^N$. Consequently, the appropriate S-mesh nodes are $\mathbb{G}^{2N} = \{\widetilde{x}_i\in[0,1] : 0=\widetilde{x}_0<\widetilde{x}_1<\cdots<\widetilde{x}_{2N-1}<\widetilde{x}_{2N}=1\}$ given as

$$\widetilde{x}_i = \begin{cases} iH_1, & \text{for} \quad 0\leq i\leq N, \\ \widetilde{x}_N + iH_2, & \text{for} \quad N+1\leq i\leq 2N. \end{cases}$$

From Theorem 3.4, the error is

$$\begin{aligned}(u-U^N)x_i &= C\left(N^{-1}\ln N\right) + O\left(N^{-1}\ln N\right), \\ &= C\left(\tfrac{N^{-1}\sigma}{\rho_0\varepsilon}\right) + O\left(N^{-1}\ln N\right),\end{aligned} \tag{4.1}$$

for $x_i\in\mathbb{G}^N$. Let $\widetilde{U}(\widetilde{x}_i)$ represent the discrete solution on the mesh $\mathbb{G}^{2N}$ (see (3.1)). From Theorem 3.4, then

$$(\widetilde{U}^N-u)\widetilde{x}_i = C\left(\tfrac{2N\sigma}{\rho_0\varepsilon}\right) + O\left(N^{-1}\ln N\right), \tag{4.2}$$

for $\widetilde{x}_i,\in\mathbb{G}^{2N}$. Now, the elimination of the $O(N^{-1})$ term from (4.1) and (4.2) leads to the following approximation

$$u(x_i) - \left(2\widetilde{U}^N - U^N\right)(x_i) = O\left(N^{-1}\ln N\right),\ x_i\in\mathbb{G}^N.$$

Therefore, we use the extrapolation formula as

$$U_{exp}(x_i) = \left(2\widetilde{U}^N - U^N\right)(x_i), \quad x_i\in\mathbb{G}^N. \tag{4.3}$$

Theorem 4.1. *Let U_{exp} represent the result of the Richardson extrapolation method (4.3) by solving the discrete problem (3.1) on two meshes $\mathbb{G}^N$ and $\mathbb{G}^{2N}$ and u be the solution of the continuous problem (1.1). Also, assume that $\varepsilon\leq N^{-1}$. Then we have the following error-bound*

$$\left|U_{exp}(x_i)-u(x_i)\right| \leq \begin{cases} CN^{-2}, & \textit{for outer layer region} \quad [0\ 1-\sigma), \\ CN^{-2}\ln^2 N, & \textit{for inner layer region} \quad [1-\sigma,\ 1]. \end{cases}$$

Proof. The error can be written in the form

$$L^N(U_{exp}-u) = L_1^N(U_{exp}-u) + L_2^N(U_{exp}-u).$$

The complete proof of error bound for $L_1^N(U_{exp}-u)$ available in [32,34,45,54],

$$\left|U_{exp}(x_i)-u(x_i)\right| \leq \begin{cases} CN^{-2}, & \text{for} \quad x_i\in(0\ 1-\sigma), \\ CN^{-2}\ln^2 N, & \text{for} \quad x_i\in[1-\sigma,\ 1). \end{cases}$$

Now, to get a bound for the L_2 operator, we write

$$L_2^N(U_{exp}-u) = L_2^N(V_{exp}-v) + L_2^N(W_{exp}-w).$$

We decompose $\widetilde{U}$ on $\mathbb{G}^{2N}$ as $\widetilde{U} = \widetilde{V} + \widetilde{W}$, where $\widetilde{W}$ is layer component and $\widetilde{V}$ is smooth layer on $\mathbb{G}^{2N}$.

Smooth component:

$$L_2^N(V_i - v_i) = L_2^N(V(x_i)) - L_2^N(v(x_i)), \quad \text{for } x_i \in \mathbb{G}^N.$$

As we have done in Theorem 3.4, taking the integral form of the Taylor series expansion and applying derivative limits, then

$$L_2^N(V_i - v_i) \le C\left(N^{-1} + N^{-2}\right),$$
$$L_2^N(V_i - v_i) \le CN^{-1} + O\left(N^{-2}\right).$$

From the stability result we can write

$$\left|(V_i - v_i)\right| \le CN^{-1} + O\left(N^{-2}\right) \quad \text{for } x_i \in \mathbb{G}^N. \tag{4.4}$$

Similarly we can obtain on $\mathbb{G}^{2N}$,

$$\left|(\widetilde{V}_i - v_i)\right| \le C(2N)^{-1} + O\left(N^{-2}\right) \quad \text{for } \widetilde{x}_i \in \mathbb{G}^{2N}. \tag{4.5}$$

Writing using the extrapolation formula (4.3) in hand

$$(V_{exp} - v)(x_i) = \Big((2\widetilde{V} - V)(x_i)\Big) - v(x_i) = \Big(2(\widetilde{V} - v) - (V - v)\Big)(x_i).$$

From (4.4) and (4.5), then

$$\left|(V_{exp} - v)(x_i)\right| = \left|\Big(2(\widetilde{V} - v) + (V - v)\Big)(x_i)\right| \le CN^{-2}.$$

Layer components:

$$L_2^N(W_i - w_i) = L_2^N(W(x_i)) - L_2^N(w(x_i)), \quad \text{for } x_i \in \mathbb{G}^N.$$

As we have done in Theorem 3.4, using the integral form of the Taylor series expansion and applying derivative limits, we have

$$L_2^N(V_i - v_i) \le C\left(N^{-1}(\ln N)^2 + N^{-2}\right),$$
$$L_2^N(W_i - w_i) \le CN^{-1}(\ln N)^2 + O\left(N^{-2}(\ln N)\right).$$

We can write from the stability result,

$$\left|(W_i - w_i)\right| \le CN^{-1}(\ln N) + O\left(N^{-2}(\ln N)^2\right) \quad \text{for } x_i \in \mathbb{G}^N. \tag{4.6}$$

Similarly we can obtain on $\mathbb{G}^{2N}$,

$$\left|(\widetilde{V}_i - v_i)\right| \le C(2N)^{-1}(\ln 2N) + O\left(N^{-2}(\ln N)^2\right) \quad \text{for } \widetilde{x}_i \in \mathbb{G}^{2N}.$$
$$\left|(\widetilde{W}_i - w_i)\right| \le C(2N)^{-2}(\ln N)^2 + O\left(N^{-2}(\ln N)^2\right) \quad \text{for } \widetilde{x}_i \in \mathbb{G}^{2N}. \tag{4.7}$$

From the extrapolation formula (4.3), we can write

$$(W_{exp} - w)(x_i) = \Big((2\widetilde{W} - W)(x_i)\Big) - w(x_i) = \Big(2(\widetilde{W} - w) - (W - w)\Big)(x_i).$$

From (4.6) and (4.7), we get

$$\left|(W_{exp} - w)(x_i)\right| = \left|\Big(2(\widetilde{W} - w) + (W - w)\Big)(x_i)\right| \le CN^{-2}(\ln N)^2.$$

Hence, we get bound on S-mesh

$$\left|U_{exp}(x_i) - u(x_i)\right| \le CN^{-2}(\ln N)^2.$$

Combining all these bounds, we get the required bound. □

5. Hybrid difference scheme (M3)

We employ the mid-point difference scheme in the coarse zone and the central finite difference scheme in the fine mesh section of this scheme, that is,

$$L^N U(x_i) = \begin{cases} \Big(-\varepsilon D_x^+ D_x^- + a_{i-\frac{1}{2}}(x_i) D^- + b(x_i) \Big) U(x_i) - \lambda \sum_{j=0}^{N} \tau_j K_{i,j} U_j = f_{i-\frac{1}{2}}, & 1 \le i \le \frac{N}{2}, \\ \Big(-\varepsilon D_x^+ D_x^- + a(x_i) D^0 + b(x_i) \Big) U(x_i) - \lambda \sum_{j=0}^{N} \tau_j K_{i,j} U_j = f_i, & \frac{N}{2} < i < N. \\ \mathcal{K}^N U_0 = U_0 - \varepsilon \sum_{i=1}^{N} \frac{g_{i-1} U i-1 + g_i U_i}{2} h_i, \\ \mathcal{K}^N U_N = U_N - \varepsilon \sum_{i=1}^{N} \frac{g_{i-1} U i-1 + g_i U_i}{2} h_i, \end{cases} \tag{5.1}$$

where $a_{i-\frac{1}{2}}(x_i) = a(\frac{x_i + x_{i-1}}{2})$.

Theorem 5.1. *Given u and U^N, which are respectively the solutions to (1.1) and (3.1), we get the following estimate of the numerical errors (3.1)*

$$\max_{1 \le i \le N-1} \Big| (u - U^N)(x_i) \Big| \le C(N^{-1} \ln N)^2.$$

Proof. It is possible to separate the discrete solution U into singular (W) and smooth (V) components. The error can be written in the form

$$L^N(U - u) = L_1^N(U - u) + L_2^N(U - u).$$

From [36], we get

$$L_1^N(U - u) \le C(N^{-1} \ln N)^2.$$

Now, for the L_2 operator, then

$$L_2^N(U - u) = L_2^N(V - v) + L_2^N(W - w) \le C(N^{-1} \ln N)^2.$$

Next, we examine the smooth and singular component bounds.

Smooth components:

$$\begin{aligned} L_2^N(V_i - v_i) &= L_2^N(V(x_i)) - L_2^N(v(x_i)), \\ &\le C \sum_{j=1}^{N} \int_{x_{j-1}}^{x_j} (x_j - \xi)(\xi - x_{j-1})(1 + |v'(\xi)| + |v''(\xi)|) d\xi, \\ &\le C N^{-2}. \end{aligned}$$

At the points $x_k = x_0$ and $x_k = x_N$, then

$$\begin{aligned} \mathcal{K}^N(V - v)(x_k) &= \mathcal{K}^N V(x_k) - \mathcal{K}^N v(x_k), \\ &= l - \mathcal{K}^N v(x_k), \\ &= v(x_k) + \varepsilon \int_{x_0}^{x_k} g(x) v(x) dx - v(x_N) - \varepsilon \sum_{i=1}^{N} \frac{g_{i-1} v_{i-1} + g_i v_i}{2} h_i, \\ |\mathcal{K}^N(V - v)(x_N)| &\le C\varepsilon((h_1^3 v''(\chi_1) + \cdots + h_N^3 v''(\chi_N)), \\ &\le C N^{-2}, \quad \text{where } \; x_{i-1} \le \chi_i \le x_i, 1 \le i \le N. \end{aligned}$$

From the stability result, then

$$|V(x_i) - v(x_i)| \le C N^{-2}.$$

Singular components:
Note that

$$|w(x_i) - W(x_i)| \le |u(x_i) - U(x_i)| + |v(x_i) - V(x_i)|.$$

Let us consider

$$\theta^{\pm}(x_i) = C N^{-2} s(x_i) \pm (U(x_i) - V(x_i)), \forall x_i \in \bar{\Omega}^{3N}.$$

Using Theorem 3.3, then

$$|U(x_i) - V(x_i)| \le CN^{-2}.$$

Now,

$$|w(x_i) - W(x_i)| \le |U(x_i) - V(x_i)| + 2|v(x_i) - V(x_i)| + |u(x_i) - v(x_i)|,$$
$$\le C_1 exp(\frac{-\alpha\sigma}{\varepsilon}) + C_1 N^{-2} \le CN^{-2}, \quad i = 0 \text{ to } \frac{3N}{4}.$$

Consider mesh functions

$$\Phi^{\pm}(x_i) = C_1 N^{-2} s(x_i) + C_1 N^{-2}\frac{\sigma}{\varepsilon^2}(x_i - (1-\sigma)) \pm (w(x_i) - W(x_i)) \quad x_i \in [1-\sigma, 1] \cap \bar{\Omega}^N,$$

where $s(x_i) = 1 + x_i$. It is easy to check $K^N \Phi^{\pm}(x_{\frac{3N}{4}}) \ge 0$ and $K^N \Phi^{\pm}(x_N) \ge 0$,

$$\mathcal{L}^N \Phi^{\pm}(x_i) \ge 0.$$

Using stability result, then $\Phi^{\pm}(x_i) \ge 0, \quad x_i \in \bar{\Omega}^N$, then

$$|w(x_i) - W(x_i)| \le CN^{-2}\ln^2 N, \quad x_i \in \bar{\Omega}^N.$$

Therefore,

$$|U(x_i) - u(x_i)| = |V(x_i) - v(x_i)| + |W(x_i) - w(x_i)| \le CN^{-2}\ln^2 N. \quad \square$$

6. Computational simulations

The suggested approach is used to solve two test problems and the results are presented in this section.

Example 6.1. Consider the following problem:

$$\begin{cases} -\varepsilon u''(x) + u'(x) + (2 - e^{-x})u(x) - 0.5\displaystyle\int_0^1 xu(s)ds = x\cos(x), \quad x \in (0,1), \\ u(0) - \varepsilon\displaystyle\int_0^1 xu(x)dx = 1, \; u(1) - \varepsilon\displaystyle\int_0^1 x^2 u(x)dx = 0. \end{cases} \tag{6.1}$$

Example 6.2. Consider the following problem:

$$\begin{cases} -\varepsilon u''(x) + \exp(-x/4)u'(x) + u(x) - 0.5\displaystyle\int_0^1 (x+s)u(s)ds = \cosh(x), \quad x \in (0,1), \\ u(0) - \varepsilon\displaystyle\int_0^1 u(x)dx = -1, \; u(1) - \varepsilon\displaystyle\int_0^1 xu(x)dx = 1. \end{cases} \tag{6.2}$$

The exact solutions of the above two examples are unknown. We apply the double mesh principle concept to get the pointwise errors and confirm the ε-uniform convergence. Let denote $\widetilde{U}^N(x_i)$, the numerical result obtained on the S-mesh created with the fixed transition parameter. This mesh is based on the $\widetilde{\mathbb{G}}^{2N}$ grid.

To determine both maximum element-wise errors for each ε as $E_\varepsilon^N = \max_{(x_i)\in\mathbb{G}^N} |U^N(x_i) - \widetilde{U}^N(x_i, t_n)|$, $E_\varepsilon^N = \max_{(x_i)\in\mathbb{G}^N} |U_{exp}^N(x_i) - \widetilde{U}_{exp}^N(x_i)|$ and is ϵ-uniform error $E^N = \max_\varepsilon E_\varepsilon^N$. The corresponding order of convergence is defined as $P_\varepsilon^N = \ln_2\left(\frac{E_\varepsilon^N}{E_\varepsilon^{2N}}\right)$. Here, the double mesh concept is also applied to the obtained extrapolation solution for $\widetilde{U}_{exp}^N(x_i)$.

Fig. 1 shows the approach of the solutions (algorithm) numerically. For different values of ε, the approximate solutions for Example 6.1 are plotted in Fig. 2 and for Example 6.2 are plotted in Fig. 3 for various values of ε on a S-mesh. These figures show that when ε decreases, boundary layers are present near $x = 1$. Solution plots of all three methods are compared in Fig. 4(a) for 10^{-2} and Fig. 4(b) for 10^{-6}. Error is plotted and compared for the three methods in Fig. 5 for 10^{-2} and 10^{-5}. From these Figures, one can

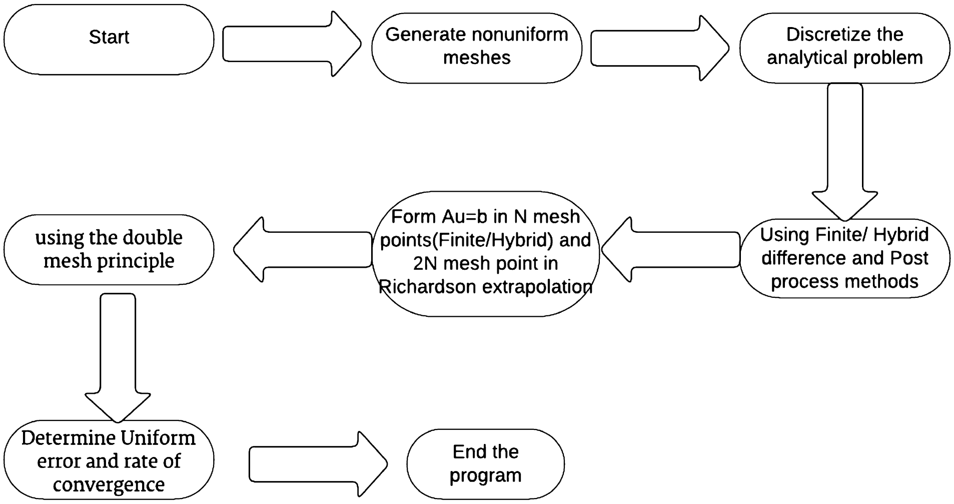

Fig. 1. Computational analysis for numerical methods.

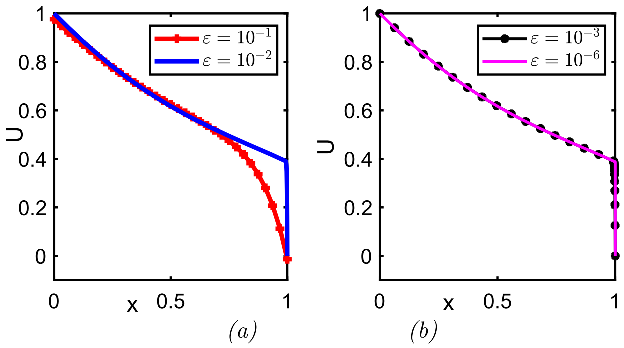

Fig. 2. Plots of the approximate solutions of Example 6.1 on the S-mesh taking $N = 64$.

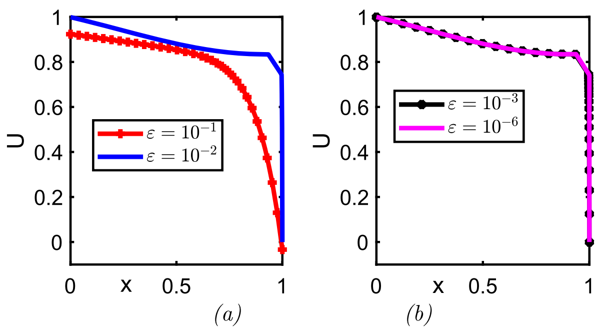

Fig. 3. Plots of the approximate solutions of Example 6.2 on the S-mesh taking $N = 64$.

observe that the error is less for the extrapolation of the upwind method than the other two methods, and using the extrapolation approach results in a decrease in the errors.

The calculated maximum pointwise errors and corresponding rate of convergence for Example 6.1 using all the proposed methods are presented in Table 1, 2, and 3. Similarly, for Example 6.2, the pointwise errors and rate of convergence are given in Table 4, 5, and 6. One can observe from these tables that the extrapolation method and hybrid method of the convergence rate is almost two (up to a logarithmic factor) on the S-mesh, but using the upwind method, the convergence rate is almost one. We note that the extrapolation accuracy is higher, but the hybrid method's convergence rate is higher. To visualize the numerical order of convergence, the maximum pointwise errors of proposed methods are plotted in a log-log scale plot on the S-mesh in Fig. 6(a) and Fig. 6(b) for Example 6.1 and Example 6.2 respectively.

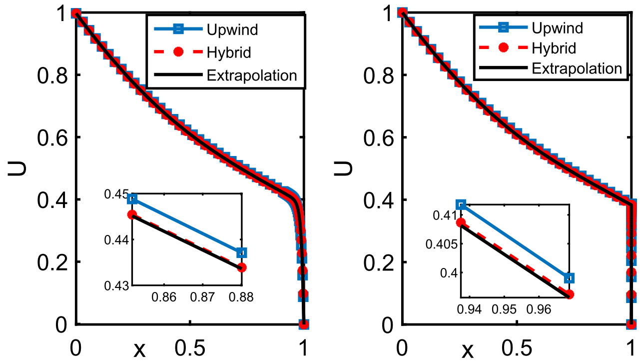

(a) *For* $\varepsilon = 10^{-2}$ (b) *For* $\varepsilon = 10^{-6}$

Fig. 4. Comparison plots of the approximate solutions of Example 6.1 on the S-mesh taking $N = 64$.

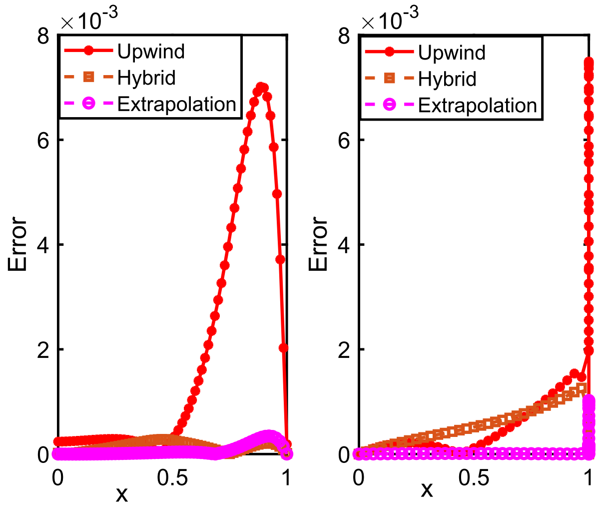

(a) *For* 10^{-2} (b) *For* 10^{-5}

Fig. 5. Comparison of Error plots for Example 6.2.

Table 1
Values of E_ε^N and P_ε^N obtained using the finite difference method for Example 6.1.

ε	Number of intervals N					
	32	64	128	256	512	1024
$1e-2$	1.1286e-2	7.5950e-3	4.8498e-3	2.9269e-3	1.7058e-3	9.6913e-4
	0.5714	0.6471	0.7285	0.7789	0.8156	
$1e-3$	1.1347e-2	7.6253e-3	4.8503e-3	2.9229e-3	1.7028e-3	9.6714e-4
	0.5734	0.6527	0.7306	0.7794	0.8161	
$1e-4$	1.1356e-2	7.6312e-3	4.8523e-3	2.9237e-3	1.7033e-3	9.6742e-4
	0.5734	0.6532	0.7308	0.7795	0.8160	
$1e-6$	1.1357e-2	7.6319e-3	4.8525e-3	2.9238e-3	1.7033e-3	9.6746e-4
	0.5734	0.6533	0.7308	0.7794	0.8160	
$1e-8$	1.1357e-2	7.6319e-3	4.8525e-3	2.9238e-3	1.7033e-3	9.6746e-4
	0.5734	0.6533	0.7308	0.7794	0.8160	
E_N	1.1357e-2	7.6319e-3	4.8525e-3	2.9269e-3	1.7058e-3	9.6913e-4
P_N	0.5735	0.6533	0.7294	0.7789	0.8157	

Remark. The present order of convergence is not optimal. In addition, it requires a prior derivative bounds which are hardly available in the literature. But if one considers aposteriori approaches given in [18,40,58] for equidistribution-based measure generations, then optimal order accuracy can be obtained.

Table 2
Values of E_ε^N and P_ε^N obtained using proposed method (M2) for Example 6.1.

ε	Number of intervals N					
	32	64	128	256	512	1024
$1e-2$	1.1004e-3	4.4740e-4	1.6689e-4	5.8072e-5	1.9138e-5	6.0604e-6
	1.2984	1.4227	1.5230	1.6014	1.6590	
$1e-3$	1.0722e-3	4.5039e-4	1.7143e-4	6.0029e-5	1.9627e-5	6.1342e-6
	1.2513	1.3936	1.5139	1.6128	1.6779	
$1e-4$	1.0365e-3	4.3418e-4	1.6518e-4	5.8294e-5	1.9457e-5	6.2408e-6
	1.2554	1.3942	1.5027	1.5831	1.6405	
$1e-6$	1.0314e-3	4.3129e-4	1.6353e-4	5.7346e-5	1.8964e-5	6.0154e-6
	1.2578	1.3991	1.5118	1.5964	1.6565	
$1e-8$	1.0313e-3	4.3126e-4	1.6351e-4	5.7335e-5	1.8957e-5	6.0111e-6
	1.2579	1.3992	1.5119	1.5967	1.6570	
E_N	1.0313e-3	4.3126e-4	1.6351e-4	5.7335e-5	1.8957e-5	6.0111e-6
P_N	1.2579	1.3992	1.5119	1.5967	1.6570	

Table 3
Values of E_ε^N and P_ε^N obtained using proposed method (M3) for Example 6.1.

ε	Number of intervals N					
	32	64	128	256	512	1024
$1e-2$	4.1541e-2	1.5074e-2	4.3665e-3	1.3415e-3	3.3609e-4	8.3768e-5
	1.4625	1.7875	1.7027	1.9969	2.0044	
$1e-3$	4.2479e-2	1.5320e-2	4.4278e-3	1.4456e-3	4.6327e-4	1.4656e-4
	1.4714	1.7907	1.6150	1.6417	1.6603	
$1e-4$	4.2556e-2	1.5350e-2	4.4401e-3	1.4580e-3	4.7016e-4	1.5013e-4
	1.4711	1.7896	1.6066	1.6328	1.6469	
$1e-6$	1.0702e-2	7.3810e-3	4.5308e-3	2.6399e-3	1.4968e-3	8.3546e-4
	1.4710	1.7895	1.6056	1.6316	1.6452	
$1e-8$	4.2564e-2	1.5354e-2	4.4416e-3	1.4596e-3	4.7103e-4	1.5059e-4
	1.4710	1.7895	1.6055	1.6316	1.6452	
E_N	4.2564e-2	1.5354e-2	4.4416e-3	1.4596e-3	4.7103e-4	1.5059e-4
P_N	1.4710	1.7895	1.6055	1.6316	1.6452	

Table 4
Values of E_ε^N and P_ε^N obtained using proposed method (M1) for Example 6.2.

ε	Number of intervals N					
	32	64	128	256	512	1024
$1e-2$	1.4569e-2	9.3638e-3	5.3313e-3	2.9033e-3	1.5721e-3	8.5531e-4
	0.6377	0.8125	8.768	8.849	8.782	
$1e-3$	1.1637e-2	8.3140e-3	5.3785e-3	3.2958e-3	1.9087e-3	1.0388e-3
	0.4851	0.6283	0.7065	0.7880	0.8777	
$1e-4$	1.0801e-2	7.4943e-3	4.6561e-3	2.7715e-3	1.6303e-3	9.6078e-4
	0.5272	0.6866	0.7484	0.7655	0.7628	
$1e-6$	1.0702e-2	7.3810e-3	4.5308e-3	2.6399e-3	1.4968e-3	8.3546e-4
	5.359	7.040	7.792	8.186	8.412	
$1e-8$	1.0701e-2	7.3798e-3	4.5295e-3	2.6385e-3	1.4952e-3	8.3371e-4
	0.5360	0.7042	0.7796	0.8193	0.8427	
E_N	1.0701e-2	7.3798e-3	4.5295e-3	2.6385e-3	1.4952e-3	8.3371e-4
P_N	0.5360	0.7042	0.7796	0.8193	0.8427	

7. Conclusion

In this article, singularly Fredholm integro-differential equations (convection-diffusion) with integral boundary conditions are solved numerically. We solved this problem numerically using three methods on Shishkin mesh. We prove that the proposed numerical schemes converge uniformly with respect to the small parameter ε, providing a first-order accuracy. Then to increase the rate of convergence, we use the post-processing technique and hybrid scheme. Hence, both methods provide a second-order convergence rate. The numerical scheme has been tested in two examples, confirming the theoretical bounds.

Table 5
Values of E_ε^N and P_ε^N obtained using proposed method (M2) for Example 6.2.

ε	Number of intervals N					
	32	64	128	256	512	1024
$1e-2$	2.1872e-3	8.2559e-4	2.9546e-4	1.0037e-4	3.2731e-5	1.0302e-5
	1.4056	1.4825	1.5576	1.6166	1.6678	
$1e-3$	2.1624e-3	9.0124e-4	3.4234e-4	1.1829e-4	3.7226e-5	1.1056e-5
	1.2627	1.3965	1.5331	1.6679	1.7515	
$1e-4$	1.9840e-3	7.9381e-4	3.0006e-4	1.0765e-4	3.7575e-5	1.2844e-5
	1.3215	1.4035	1.4789	1.5185	1.5486	
$1e-6$	1.9566e-3	7.7208e-4	2.8664e-4	9.8835e-5	3.2431e-5	1.0715e-5
	1.3415	1.4295	1.5362	1.6076	1.6611	
$1e-8$	1.9563e-3	7.7185e-4	2.8649e-4	9.8730e-5	3.2356e-5	1.0200e-5
	1.3417	1.4298	1.5369	1.6095	1.6654	
E_N	1.9563e-3	7.7185e-4	2.8649e-4	9.8730e-5	3.2356e-5	1.0200e-5
P_N	1.3417	1.4298	1.5369	1.6095	1.6654	

Table 6
Values of E_ε^N and P_ε^N obtained using proposed method (M3) for Example 6.2.

ε	Number of intervals N					
	32	64	128	256	512	1024
$1e-2$	4.4617e-2	1.4413e-2	4.6012e-3	1.4519e-3	4.3662e-4	1.0686e-4
	1.6302	1.6473	1.6641	1.7335	2.0306	
$1e-3$	4.4222e-2	1.3960e-2	4.3341e-3	1.3122e-3	3.8445e-4	1.0410e-4
	1.6635	1.6875	1.7238	1.7711	1.8848	
$1e-4$	4.4172e-2	1.3887e-2	4.2810e-3	1.2814e-3	3.6532e-4	9.4270e-5
	1.6694	1.6977	1.7402	1.8105	1.9543	
$1e-6$	4.4166e-2	1.3879e-2	4.2746e-3	1.2777e-3	3.6299e-4	9.3077e-5
	1.6701	1.6990	1.7423	1.8155	1.9634	
$1e-8$	4.4166e-2	1.3878e-2	4.2746e-3	1.2776e-3	3.6296e-4	9.3065e-5
	1.6701	1.6990	1.7423	1.8155	1.9634	
E_N	4.4166e-2	1.3878e-2	4.2746e-3	1.2776e-3	3.6296e-4	9.3065e-5
P_N	1.6701	1.6990	1.7423	1.8155	1.9634	

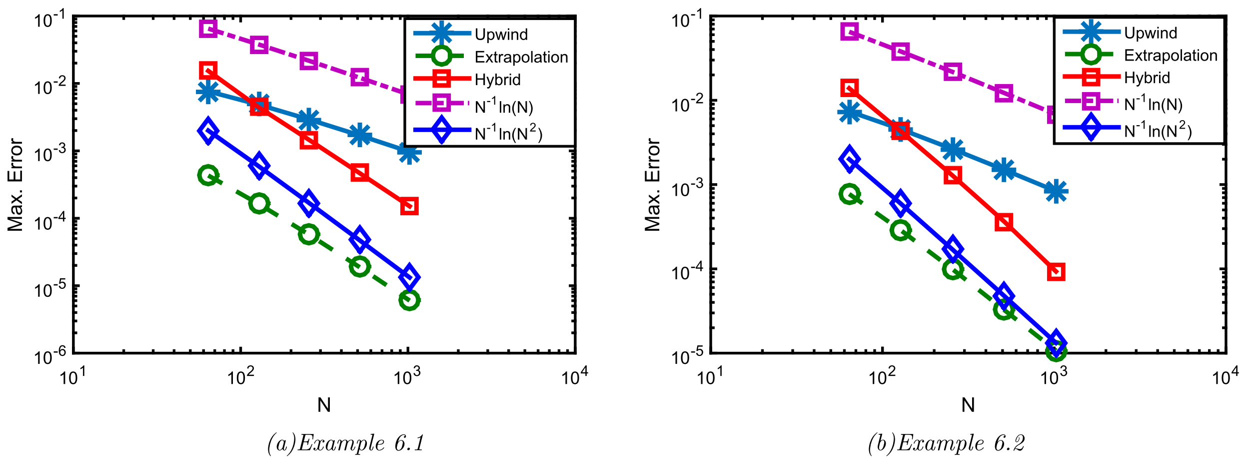

Fig. 6. Comparison of Log-log plot for 10^{-6}.

Availability of supporting data

Not applicable.

Funding

Not applicable.

Ethical approval

Not applicable.

CRediT authorship contribution statement

Sekar Elango: Writing – review & editing, Writing – original draft, Supervision, Methodology, Conceptualization. **L. Govindarao:** Writing – review & editing, Writing – original draft, Visualization, Validation. **R. Vadivel:** Writing – review & editing, Investigation.

Declaration of competing interest

The authors declare that they have no competing interests concerning the publication of the manuscript.

Acknowledgement

The authors express their gratitude to the referees for their helpful and constructive comments.

References

[1] G.M. Amiraliyev, M.E. Durmaz, M. Kudu, Uniform convergence results in singularly perturbed Fredholm integro-differential equations, J. Math. Anal. 9 (6) (2018) 55–64.
[2] G.M. Amiraliyev, S. Sevgin, Uniform difference method for singularly perturbed Volterra integro-differential equations, Appl. Math. Comput. 179 (2006) 731–741.
[3] H. Brunner, P. van der, The Numerical Solution of Volterra Equations CWI Monographs, NorthHolland, Amsterdam, 1986.
[4] H. Brunner, Numerical Analysis and Computational Solution of Integro-Differential Equations, Springer, Cham, 2018.
[5] M. Cakır, B. Gunes, A new difference method for the singularly perturbed Volterra-Fredholm integro-differential equations on a Shishkin mesh, Hacet. J. Math. Stat. 51 (3) (2022) 787–799.
[6] E. Cimen, M. Cakir, A uniform numerical method for solving singularly perturbed Fredholm integro-differential problem, Comput. Appl. Math. 40 (42) (2021) 1–14.
[7] J. Chen, M. He, T. Zeng, A multiscale Galerkin method for second-order boundary value problems of Fredholm integro-differential equation II: efficient algorithm for the discrete linear system, J. Vis. Commun. Image Represent. 58 (2019) 112–118.
[8] J. Chen, M. He, Y. Huang, A fast multiscale Galerkin method for solving second order linear Fredholm integro-differential equation with Dirichlet boundary conditions, J. Comput. Appl. Math. 364 (2020) 112352.
[9] P. Das, A higher order difference method for singularly perturbed parabolic partial differential equations, J. Differ. Equ. Appl. 24 (3) (2018) 452–477.
[10] P. Das, An a posteriori based convergence analysis for a nonlinear singularly perturbed system of delay differential equations on an adaptive mesh, Numer. Algorithms 81 (2019) 465–487.
[11] A. Das, L. Govindarao, J. Mohapatra, A second order weighted monotone numerical scheme for time-delayed parabolic initial-boundary-value problem involving a small parameter, Int. J. Math. Model. Numer. Optim. 12 (3) (2022) 233–251.
[12] P. Das, S. Natesan, Richardson extrapolation method for singularly perturbed convection-diffusion problems on adaptively generated mesh, CMES Comput. Model. Eng. Sci. 90 (6) (2013) 463–485.
[13] A. Das, S. Natesan, Uniformly convergent numerical method for singularly perturbed 2D delay parabolic convection-diffusion problems on Bakhvalov-Shishkin mesh, Int. J. Math. Model. Numer. Optim. 8 (4) (2018) 305–330.
[14] P. Das, S. Rana, Theoretical prospects of fractional order weakly singular Volterra integro differential equations and their approximations with convergence analysis, Math. Methods Appl. Sci. 44 (2021) 9419–9440.
[15] P. Das, S. Rana, H. Ramos, A perturbation-based approach for solving fractional-order Volterra–Fredholm integro-differential equations and its convergence analysis, Int. J. Comput. Math. 97 (10) (2020) 1994–2014.
[16] P. Das, S. Rana, H. Ramos, Homotopy perturbation method for solving Caputo-type fractional-order Volterra-Fredholm integro-differential equations, Comput. Math. Methods 1 (2019) e1047.
[17] P. Das, S. Rana, J. Vigo-Aguiar, Higher order accurate approximations on equidistributed meshes for boundary layer originated mixed type reaction diffusion systems with multiple scale nature, Appl. Numer. Math. 148 (2020) 79–97.
[18] P. Das, Comparison of a priori and a posteriori meshes for singularly perturbed nonlinear parameterized problems, J. Comput. Appl. Math. 290 (2015) 16–25.
[19] P. Das, J. Vigo-Aguiar, Parameter uniform optimal order numerical approximation of a class of singularly perturbed system of reaction diffusion problems involving a small perturbation parameter, J. Comput. Appl. Math. 354 (2019) 533–544.
[20] P. Das, S. Rana, H. Ramos, On the approximate solutions of a class of fractional order nonlinear Volterra integro-differential initial value problems and boundary value problems of first kind and their convergence analysis, J. Comput. Appl. Math. 404 (2022) 113116.
[21] M.C. De Bonis, D. Occorsio, W. Themistoclakis, Filtered interpolation for solving Prandtl's integro-differential equations, Numer. Algorithms 88 (2021) 679–709.
[22] M.C. De Bonis, A. Mennouni, D. Occorsio, A numerical method for solving systems of hypersingular integro-differential equations, Electron. Trans. Numer. Anal. 58 (2023) 378–393.
[23] A. De Gaetano, O. Arino, Mathematical modeling of the intravenous glucose tolerance test, J. Math. Biol. 40 (2000) 136–168.
[24] G. De Marsily, Quantitative Hydrogeology – Groundwater Hydrology for Engineers, Academic Press, Orlando, Florida, 1986.
[25] M.E. Durmaz, G.M. Amiraliyev, A robust numerical method for a singularly perturbed Fredholm integro-differential equation, Mediterr. J. Math. 18 (24) (2021) 1–17.
[26] M.E. Durmaz, M. Cakır, I. Amirali, G.M. Amiraliyev, Numerical solution of singularly perturbed Fredholm integro-differential equations by homogeneous second-order difference method, J. Comput. Appl. Math. 412 (2022) 114327.
[27] M.E. Durmaz, M. Cakır, G. Amiraliyev, Parameter uniform second-order numerical approximation for the integro-differential equations involving boundary layers, Commun. Fac. Sci. Univ. Ank. Sér. A1 Math. Stat. 71 (4) (2022) 954–967.
[28] M.E. Durmaz, G. Amiraliyev, M. Kudu, Numerical solution of a singularly perturbed Fredholm integro-differential equation with Robin boundary condition, Turk. J. Math. 46 (1) (2022) 207–224.
[29] M.E. Durmaz, I. Amirali, G.M. Amiraliyev, An efficient numerical method for a singularly perturbed Fredholm integro-differential equation with integral boundary condition, J. Appl. Math. Comput. 69 (1) (2023) 505–528.
[30] S. Elango, L. Govindarao, J. Mohapatra, R. Vadivel, N. Hu, Numerical analysis for second order differential equation of reaction-diffusion problems in viscoelasticity, Alex. Eng. J. 92 (2024) 92–101.

[31] A. Fahim, M.A.F. Araghi, Numerical solution of convection-diffusion equations with memory term based on sinc method, Comput. Methods Differ. Equ. 6 (3) (2018) 380–395.
[32] J. Mohapatra, L. Govindarao, A fourth-order optimal numerical approximation and its convergence for singularly perturbed time delayed parabolic problems, Iran. J. Numer. Anal. Optim. 12 (2) (2021) 250–276.
[33] L. Govindarao, H. Ramos, S. Elango, Numerical scheme for singularly perturbed Fredholm integro-differential equations with non-local boundary conditions, Comput. Appl. Math. 43 (3) (2024) 126.
[34] J.L. Gracia, C. Clavero, Richardson extrapolation on generalized Shishkin meshes for singularly perturbed problems, Monogr. Semin. Mat. García Galdeano 31 (2004) 169–178.
[35] R. Grimmer, J.H. Liu, Singular perturbations in viscoelasticity, Rocky Mt. J. Math. 24 (1994).
[36] P. Hammachukiattikul, E. Sekar, A. Tamilselvan, R. Vadivel, N. Gunasekaran, Praveen Agarwa, Comparative study on numerical methods for singularly perturbed advanced-delay differential equations, J. Math. (2021) 6636607.
[37] R. Jalilian, T. Tahernezhad, Exponential spline method for approximation solution of Fredholm integro-differential equation, Int. J. Comput. Math. 97 (4) (2020) 791–801.
[38] A. Jerri, Introduction to Integral Equations with Applications, Wiley, New York, 1999.
[39] M. Kudu, I. Amirali, G.M. Amiraliyev, A finite-difference method for a singularly perturbed delay integro-differential equation, J. Comput. Appl. Math. 308 (2016) 379–390.
[40] K. Kumar, P.C. Podila, P. Das, H. Ramos, A graded mesh refinement approach for boundary layer originated singularly perturbed time-delayed parabolic convection diffusion problems, Math. Methods Appl. Sci. 44 (16) (2021) 12332–12350.
[41] C.G. Lange, D.R. Smith, Singular perturbation analysis of integral equations: part II, Stud. Appl. Math. 90 (1) (1993) 1–74.
[42] A.S. Lodge, J.B. McLeod, J.A.A. Nohel, Nonlinear singularly perturbed Volterra integro-differential equation occurring in polymer rheology, Proc. R. Soc. Edinb., Sect. A 80 (1978) 99–137.
[43] A. Mennouni, Improvement by projection for integro-differential equations, Math. Methods Appl. Sci. (2020), https://doi.org/10.1002/mma.6318.
[44] J.J.H. Miller, E. O'Riordan, I.G. Shishkin, Fitted Numerical Methods for Singular Perturbation Problems, World Scientific, Singapore, 1996.
[45] M.C. Natividad, M. Stynes, Richardson extrapolation for a convection–diffusion problem using a Shishkin mesh, Appl. Numer. Math. 45 (2003) 315–329.
[46] N.N. Nefedov, A.G. Nikitin, The asymptotic method of differential inequalities for singularly perturbed integro-differential equations, Differ. Equ. 36 (10) (2000) 1544–1550.
[47] N.N. Nefedov, A.G. Nikitin, The Cauchy problem for a singularly perturbed integro-differential Fredholm equation, Comput. Math. Math. Phys. 47 (4) (2007) 629–637.
[48] A. Saadatmandi, M. Dehghan, Numerical solution of the higher-order linear Fredholm integro-differential-difference equation with variable coefficients, Comput. Math. Appl. 59 (2010) 2996–3004.
[49] E. Sekar, Second order singularly perturbed delay differential equations with non-local boundary condition, J. Comput. Appl. Math. 417 (2023) 114498.
[50] E. Sekar, A. Tamilselvan, Singularly perturbed delay differential equations of convection–diffusion type with integral boundary condition, J. Appl. Math. Comput. 59 (1) (2019) 701–722.
[51] E. Sekar, A. Tamilselvan, R. Vadivel, Nallappan Gunasekaran, Haitao Zhu, Jinde Cao, Xiaodi Li, Finite difference scheme for singularly perturbed reaction diffusion problem of partial delay differential equation with non local boundary condition, Adv. Differ. Equ. 1 (2021) 1–20.
[52] E. Sekar, A. Tamilselvan, Parameter uniform method for a singularly perturbed system of delay differential equations of reaction–diffusion type with integral boundary conditions, Int. J. Appl. Math. 5 (3) (2019) 1–12.
[53] G.I. Shishkin, L.P. Shishkina, Difference Methods for Singular Perturbation Problems, CRC Press, Boca Raton, 2009.
[54] G.I. Shishkin, L.P. Shishkina, Difference scheme of highest accuracy order for a singularly perturbed reaction–diffusion equation based on the solution decomposition method, Proc. Steklov Inst. Math. 292 (1) (2016) 262–275.
[55] S.S. Siddiqi, S. Arshed, Numerical solution of convection-diffusion integro-differential equations with a weakly singular kernel, J. Basic Appl. Sci. Res. 3 (11) (2013) 106–120.
[56] H.M. Srivastava, A.K. Nain, R.K. Vats, P. Das, A theoretical study of the fractional-order p-Laplacian nonlinear Hadamard type turbulent flow models having the Ulam–Hyers stability, Rev. R. Acad. Cienc. Exactas Fís. Nat., Ser. A Mat. 117 (2023) 160.
[57] S. Saini, P. Das, S. Kumar, Parameter uniform higher order numerical treatment for singularly perturbed Robin type parabolic reaction diffusion multiple scale problems with large delay in time, Appl. Numer. Math. 196 (2024) 1–21.
[58] S. Saini, P. Das, S. Kumar, Computational cost reduction for coupled system of multiple scale reaction diffusion problems with mixed type boundary conditions having boundary layers, Rev. R. Acad. Cienc. Exactas Fís. Nat., Ser. A Mat. 117 (2) (2023) 66.
[59] S. Santra, J. Mohapatra, P. Das, D. Choudhuri, Higher order approximations for fractional order integro-parabolic partial differential equations on an adaptive mesh with error analysis, Comput. Math. Appl. 150 (2023) 87–101.
[60] D. Shakti, J. Mohapatra, P. Das, Jesus Vigo-Aguiar, A moving mesh refinement based optimal accurate uniformly convergent computational method for a parabolic system of boundary layer originated reaction–diffusion problems with arbitrary small diffusion terms, J. Comput. Appl. Math. 404 (2022) 113167.
[61] R. Shiromani, V. Shanthi, P. Das, A higher order hybrid-numerical approximation for a class of singularly perturbed two-dimensional convection-diffusion elliptic problem with non-smooth convection and source terms, Comput. Math. Appl. 142 (2023) 9–30.